NEOPLASIA
www.neoplasia.com

Volume 19 Number 5 May 2017 pp. 396–411 396

Specific microRNA–mRNA Regulatory Network of Colon Cancer Invasion Mediated by Tissue Kallikrein–Related Peptidase 6[1]

Earlphia Sells*, Ritu Pandey†,‡, Hwudaurw Chen†, Bethany A. Skovan†, Haiyan Cui† and Natalia A. Ignatenko‡

*Biochemistry and, Molecular and Cellular Biology Graduate Program, Department of Molecular and Cellular Biology, College of Science, University of Arizona, Tucson, AZ, USA; †University of Arizona, Cancer Center, University of Arizona, Tucson, AZ, USA; ‡Department of Cellular and Molecular Medicine, University of Arizona, Tucson, AZ, USA

Abstract

Metastatic colon cancer is a major cause of deaths among colorectal cancer (CRC) patients. Elevated expression of kallikrein 6 (KLK6), a member of a kallikrein subfamily of peptidase S1 family serine proteases, has been reported in CRC and is associated with low patient survival rates and poor disease prognosis. We knocked down KLK6 expression in HCT116 colon cancer cells to determine the significance of KLK6 expression for metastatic dissemination and to identify the KLK6-associated microRNAs (miRNAs) signaling networks in metastatic colon cancer. KLK6 suppression resulted in decreased cells invasion in vitro with a minimal effect on the cell growth and viability. In vivo, animals with orthotopic colon tumors deficient in KLK6 expression had the statistically significant increase in survival rates ($P = .005$) and decrease in incidence of distant metastases. We further performed the integrated miRNA and messenger RNA (mRNA) expression profiling to identify functional miRNA-mRNA interactions associated with KLK6-mediated invasiveness of colon cancer. Through bioinformatics analysis we identified and functionally validated the top two up-regulated miRNAs, miR-182 and miR-203, and one down-regulated miRNA, miRNA-181d, and their seven mRNA effectors. The established miRNA-mRNA interactions modulate cellular proliferation, differentiation and epithelial–mesenchymal transition (EMT) in KLK6-expressing colon cancer cells via the TGF-β signaling pathway and RAS-related GTP-binding proteins. We confirmed the potential tumor suppressive properties of miR-181d and miR-203 in KLK6-expressing HCT116 cells using Matrigel invasion assay. Our data provide experimental evidence that KLK6 controls metastasis formation in colon cancer via specific downstream network of miRNA-mRNA effectors.

Neoplasia (2017) 19, 396–411

Introduction

Metastases present the main cause of mortality in cancer patients. The 5-year survival of patients with CRC drops from 90%, if cancer is detected at localized stage, to 68% if the cancer cells have spread regionally to involve adjacent organs and/or lymph nodes [1]. Despite improvements in early detection and screening, about 20% of patients with CRC present at the incurable metastatic stage.

Although significant progress has been made in identifying a number of key molecules contributing the process of tumor growth and metastatic invasion, the efforts to block cancer metastasis remain

Abbreviations: CRC, colorectal cancer; KLK6, kallikrein-related peptidase 6; EMT, epithelial- mesenchymal transition; FOS, FBJ murine osteosarcoma viral oncogene homolog; PAM, peptidylglycine alpha-amidating monooxygenase; *VCAN*, versican; EHF, *Ets* homologous factor; HMGA2, high-mobility group AT-hook 2; GAPDH, glyceraldehyde 3′-phosphate dehydrogenase; RIT1, *Ric*-related gene expressed throughout the organism; RUNX2, transforming growth factor beta 2 (TGF-β2) Runt–related transcription factor 2

Address all correspondence to: Natalia Ignatenko, Arizona Cancer Center, 1515 N. Campbell Ave, Rm 3985, Tucson, AZ, 85724.
E-mail: nai@email.arizona.edu

[1] Grant Acknowledgement: National Institutes of Health Grants RO1CA157595, 3R01CA157595-03S1 (Research Supplement to promote diversity in health-related research) and 5P30CA23074-32 (The University of Arizona Cancer Center Support Grant) and The University of Arizona/Sloan Indigenous Graduate Partnership Fellowship 4301-62780.
Received 15 December 2016; Revised 2 February 2017; Accepted 6 February 2017

1476-5586
http://dx.doi.org/10.1016/j.neo.2017.02.003

a challenging step in treating cancer. The invasion-metastasis cascade includes several important steps starting with local invasion of cancer cells from the primary site into surrounding tumor-associated stroma, following intravasation into the lumina of lymphatic or blood vessels, cell survival during circulation, and initiation of tumor cells parenchyma, and growth within blood vessel into the tissue (extravasation) [2]. The list of molecular mediators of the different steps in invasion-metastasis cascade has expanded significantly to include, in addition to the known genetic and epigenetic events, also the different classes of small non-protein coding regulatory RNAs, such as microRNAs (miRNAs), small nucleolar RNAs (snoRNAs), short interfering RNAs (siRNAs) and small double-stranded RNAs [2–4]. MicroRNAs are 19- to 25-nucleotide-length non-coding RNAs, which negatively regulate gene expression post- transcriptionally through imperfect binding to the 3′ untranslated region (3′UTR) of target messenger RNA leading to inhibition of translation and mRNA destabilization [5,6]. MicroRNAs are dysregulated in many cancers, including colorectal cancer, and can act as tumor suppressors or oncogenes, depending on their targets [7–9]. A number of miRNA networks that function in a synergistic manner to control different cellular pathways have been under investigation [10,11].

Growing evidence indicates that the members of a human tissue kallikrein-related peptidases family of 15 serine proteases, which have diverse physiological functions, are associated with malignancy and have the diagnostic/prognostic applications in cancer [12–14]. The role of kallikreins in cancer pathogenesis is related to their ability to degrade the extracellular matrix proteins and promote angiogenesis [12]. Human kallikrein-related peptidase 6 (*KLK6*) gene (by old nomenclature protease M/zyme/neurosin) is a member of the human tissue kallikrein family [15]. Biochemical and structural studies show that human KLK6 protein is an active serine protease [16]. *KLK6* mRNA expression is elevated in malignant colorectal tissues compared with non-malignant ones and correlates with serosal invasion, liver metastasis, advanced Duke's stage, and a poor prognosis [17–19]. The bioinformatics analysis of expression data from a cohort of colorectal cancer patients, identified the KLK6 gene as one of the top six up-regulated genes associated with the survival of colorectal cancer patients through metastasis related signaling pathways [20]. The mechanism of regulation of KLK6 expression in colon cancer is not fully investigated. Nevertheless, alterations in major cancer driver genes, such as K-RAS oncogene and APC tumor suppressor gene, may contribute to KLK6 up-regulation in colon cancer [21,22]. The possibility of post-transcriptional regulation of KLK6 by microRNAs, i.e., miRNA let-7f, has been also reported [11,23]. Here we investigated the miRNA-based mechanism of regulation of invasion in KLK6-expressing colon cancer cells with high metastatic potential. We have designed the specific KLK6-mediated miRNA-mRNA network which regulates the expression of genes controlling cellular proliferation, differentiation and epithelial-mesenchymal transition (EMT) through TGF-β signaling pathway and RAS-related GTP-binding proteins.

Materials and methods

Cell lines

The HCT116 parental cells, HCT116 Control and shKLK6 cell lines (described in more details below) were used in this study. HCT116 parental cells were maintained in Dulbecco's Modified Eagle Medium (DMEM) with 4.5 mg/L glucose, L-glutamine w/o sodium pyruvate, supplemented with 10% FBS and 1% penicillin/streptomycin. HCT116 Control and shKLK6 cells were maintained in DMEM media described above with addition of selection marker puromycin at the concentration of 0.5 μg/ml of media (Thermo Fisher Scientific, Inc.).

Generation of HCT116 Isogenic Cells with KLK6 Knockdown

In order to knock down *KLK6* expression, SureSilencing short-hairpin RNA plasmids targeting four different regions of the *KLK6* gene (shKLK6 plasmids), as well as a negative control plasmid expressing a scrambled shRNA sequence, were used (SureSilencing shRNAs, Qiagen, Inc.) (Supplementary Figure 1*A*). Plasmids were transfected into HCT116 colon cancer cell line using LipofectAMINE 2000 according to the manufacturer's instructions. Forty-eight hours after transfection cells were switched to selection medium containing 0.5 μg/ml puromycin. Selection medium was changed every two days until only cells expressing control and shKLK6 plasmids grew. Initial screening of HCT116 shKLK6 isogenic cell lines was done using quantitative RT PCR (qPCR) and KLK6 ELISA.

Cell Growth

HCT116 control clone 1 and shKLK6 clones were plated in six-well plates at a concentration of 0.1×10^6 cells/well and incubated for 37°C in 5% CO_2. All cells were plated in triplicate. The cells were grown for at least 10 days. The cells were harvested and total cell concentration and viability were determined using the trypan blue dye exclusion method on a Vi-Cell Series Cell Viability Analyzer (Beckman Coulter, Inc.). Determination of population doubling time was performed by plotting viable cell number vs. time (days). Data were derived from three independent experiments.

RNA Isolation

Total RNA was extracted from HCT116 Control and shKLK6 clones 48 hours after subculture using miRVana miRNA isolation kit (Ambion, Austin, TX). RNA purity was assessed using a Nanodrop spectrophotometer (ND-2000; Thermo Scientific, Pittsburgh, PA). All RNA samples prepared for experiments had 260/280 absorption values between 1.8 and 2.0. Integrity of the isolated RNA was also evaluated by using a standard 1% formaldehyde agarose gel and confirmed by using the Agilent Technologies' 2100 Bioanalyzer (Agilent Technologies). The RNA Integrity (RIN) Numbers generated were between 8.5 and 10 (Intact and non-fragmented RNA) (UA Genomic Core Facility).

Microarray Hybridization

Affymetrix Human ST 1.0 array and Affymetrix miRNA 2.0 chips were used to quantify mRNA and miRNA in total RNA from the HCT116 Control clone 1 cells and shKLK6-3 clone 3 cells. RNA labeling and hybridization, as well as array processing and scanning were performed by Asuragen, Inc., using standard procedures with normalization performed using the Variance Stabilization Normalization (VSN) method.

mRNA and miRNA Data Processing

Raw data files from gene ST 1.0 array hybridization were processed using BioConductor [24] Affymetrix modules to perform background subtraction and quantile normalization using the Robust MultiChip Algorithm (RMA). Quality control analysis was performed on the chips that included correlation plots, density plots, box plots and

RNA degradation analysis. Analysis of Variance was used to estimate differential mRNA expression between samples using the BioConductor Limma module [25]. Limma analysis provides an empirical Bayesian method to improve variance estimation and corrects for multiple hypothesis testing by the Benjamini Hochburg False Discovery Rate method. mRNA with adjusted *P* values lower than .05 and log odds score provided by B-statistics greater than 3.0 were considered significantly changing. miRNA differential expression analysis between two groups was done using statistical analysis of variance test by Asuragen, Inc., and miRNAs with *P* value lower than .05 were considered significant.

Quantitative Real-time PCR

Total RNA was isolated as described above. Reverse transcription to produce cDNA template was completed using the Applied Biosystems High Capacity cDNA Reverse Transcription Kit (Part #4368814). qPCR was performed using Taqman® probes (Applied Biosystems) specific for the mRNAs of interest: KLK6 (Hs00160519_m1), EHF (Hs00171917_m1), RIT1 (Hs00608424_m1), TGF-β (Hs00234244_m1), BAMBI (Hs03044164_m1), PAM (Hs00168596_m1), RUNX2 (Hs1047973_m1), FOS (Hs04194186_m1), VCAN (Hs0171642_m1). 0.2 μg of total RNA was transcribed into cDNA in a 20 μl reaction with random hexamers under thermal condition recommended by the protocol. Real-time PCR amplification was performed with the ABI PRISM 7700 SDS instrument (Applied Biosystems, Life Technologies Inc.), under the universal thermal cycling conditions recommended by the Assay-on-Demand products protocol. Each 20 μl real-time PCR reaction included 10 μl of 2× TaqMan Universal PCR master mix, 4 μl of the resulting cDNA from the reverse transcription step, and 6 μl diluted primer and probe mixes ordered from Assay-on-Demand gene expression assay mix (Applied Biosystems). Negative controls without template were included in each plate to monitor potential PCR contamination. The expression of genes was tested in triplicate and each reaction was run in duplicate. To determine the relative expression level of each target gene, the comparative *CT* method was used. The *CT* value of the target gene was normalized by the endogenous reference β 2-microglobin (β 2 M, FAM (Hs99999907_m1)) was used as the endogenous reference. The relative expression of each target gene was calculated via the equation $2^{-\Delta\Delta C}{}_T$ where $\Delta C_T = C_{T(\text{target})} - C_{T(\beta 2M)}$. Data were analyzed using a *t*-test when comparing two groups.

For the analysis of miRNA alteration levels, 5 ng of extracted total RNA was reverse transcribed using Applied Biosystems miRNA Reverse Transcription Kit and sequence- specific stem-loop primers (Applied Biosystems), which target the mature miRNA sequence. qPCR was performed using Taqman® probes (Applied Biosystems) specific for the miRNAs of interest: hsa-miR-181d (TM:001099), –miR-182 (TM:000483), –miR-203 (TM:000507). In brief, each 20 μl reaction included 10 μl of 2× Taqman Universal master mix with no AmpErase UNG, 1.33 μl of the resulting product from the RT reaction, and 1 μl 20× Taqman small RNA assay. qPCR was performed with the ABI PRISM 7700 SDS instrument (Applied Biosystems), under the universal thermal cycling conditions. Controls without template were included in each plate. All reactions were performed in triplicate. To determine the relative expression level of each target gene, the comparative C_T method was used. The C_T value of the target gene was normalized by the endogenous reference. RNU38B (SNORD38B, RT:001004) was used as the endogenous reference. The relative expression of each target gene was calculated via the equation $2^{-\Delta C}{}_T$, where $\Delta C_T = C_{T(\text{target})} - C_{T(\text{RNU38B})}$. Data were analyzed using a Student's *t*-test when comparing two groups and one-way ANOVA. The significance level of statistics was set at $P = .05$.

Western Analysis

Cells were harvested by trypsinizing for 2 minutes and subsequently pelleting at 1000 X g for 5 minutes at 4°C. Cells were washed (3×) with ice-cold PBS, lysed on ice (30 minutes) in RIPA lysis buffer (PBS, 1% NP-40, 0.5% sodium deoxycholate, 0.1% SDS) with 1 tablet Complete Mini protease inhibitor and 1 tablet PhosohoSTOP (30 μg/ml aprotinin, 100 mM sodium orthovanidate and 10 mg/ml phenylmethylsulfonyl fluoride at 1 tablet each per 10 ml RIPA lysate; Roche), and scraped into microcentrifuge tubes. Total proteins in the supernatant were isolated by centrifugation (10,000×*g*, 4°C) for 10 minutes and quantitatively analyzed by using the Bio-Rad DC protein assay kit. Equal amounts (50 μg) of the protein were separated on Mini-PROTEAN TGX Bio-Rad Precast Gels Any-kD (Criterion TGX Stain-free, Cat#5678123; Bio-Rad laboratories, Inc.) and transferred to Hybond-C nitrocellulose membrane (GE Healthcare Life Sciences) for 1 hour. After blocking with Blotto A (5% w/v non-fat milk, 0.1% Tween 20, and Tris-buffered saline (TBS) consisting of 10 mM Tris–HCl, pH 8.0, 150 mM NaCl) for 1 hour at room temperature. The primary and secondary antibodies used in this study and blotting conditions are presented in Supplementary Table 1. The primary antibodies were incubated with the membrane (blot) overnight at 4°C. The blots were washed in TBS/0.05% Tween-20. Proteins of interest were detected with an enhanced chemiluminescent detection reagent (Thermo Scientific Super Signal West Pico or West Femto Chemiluminescent Substrate, Cat#34077 or 34,095, respectively) and exposed to film (Denville Scientific Inc., HyBlot CL, Autoradiography film, Cat#E3012).

All Western blots were repeated at least two times. Image processing program, Image J (NIH) was used for evaluation of western blot bands intensity where specified (Image J, http://rsb.info.nih.gov/ij/docs/menus/analyze.html#gels). Bands of the protein of interest were normalized to β-actin.

KLK6 ELISA

An ELISA kits for the detection of human KLK6 in conditioned media were obtained from IBEX (Quebec, Canada) and, after this product was discontinued, from Boster Biological Technology Co., Ltd. (Pleasanton, CA, Cat# EK0818). The assays were performed according to manufacturer's instructions. The detection range for these kits is: 0.2 to 20 ng/ml (IBEX) and 0.078 to 5 ng/ml (Boster Biological). KLK6 antigen levels are expressed as nanograms per milliliter. The plate was read at 490 nm on an EL800 Universal Microplate Reader (Bio-Tek Instruments, Inc., Winooski, VT). In each experiment samples were analyzed in triplicates and all experiments were repeated two or three times. Detection of KLK6 secreted in the serum of SCID animals injected with HCT116 control clone 1 and shKLK6 clone 3 was done by ELISA in the Laboratory of Dr. Eleftherios P. Diamandis, at the Advanced Centre for Detection of Cancer (ACDC) (www.acdclab.org, University of Toronto, Canada).

Cell Migration/invasion Assay

HCT116 Control clone 1 and shKLK6 clones 1 to 3 were seeded in 24-well chambers with either control plastic inserts or Matrigel coated inserts with a 0.8 μm pore size (Corning Inc., Corning, NY).

In the lower chamber of each well 0.5 ml of media with 10% FBS was added as a chemoattractant. Cell suspension was prepared at a concentration of 0.5×10^6 cells/ml in serum-free medium. 200 µl of cell suspensions (1×10^5 cells) was plated into inserts. The cells were allowed to migrate/invade for 48 hours. The media were discarded and inserts were rinsed briefly with 1× PBS and swabbed gently with a cotton tip inside inserts to remove non-migrating or non-invading cells. Subsequently, migrating/invading cells were fixed in 100% methanol for 2 minutes, stained with 1% toluidine blue in 1% borax) for 2 minutes, rinsed twice in ddH_2O, swabbed gently again inside with a cotton tip and air-dried. Control inserts were included following similar treatment. The stained membranes were cut from the inserts and the incorporated toluidine blue was dissolved in 200 µl of 0.1 M citric acid in a 96-well plate while shaking for 5 minutes on a high-speed titer plate shaker and quantified at 560 nm. The samples were transferred to a new 96-well plate and read at 560 nm on a Synergy 2 Multi-Detection Microplate Reader (Bio-Tek Instruments, Inc.,Winooski, VT). Each migration/invasion experiment was carried out in sextuplet and was repeated twice.

In Vitro KLK6 Rescue Experiment

The pcDNA3.1 KLK6 plasmid, expressing enzymatically active KLK6 [26] was generously provided by Dr. Georgios Pampalakis and Dr. Georgia Sotiropoulou, Department of Pharmacy, University of Patras, Greece. Control clone 1 and shKLK6 clone 3 cells were seeded in 100 mm^2 Petri dishes at the concentration of 1.2×10^6 cells. Twenty-four hours after subculture cells were transfected with pcDNA 3.1 KLK6 plasmid or empty pCDNA3.1 using LipofectAMINE 2000 reagent according to the manufacturer's instructions. Twenty-four hours after transfection (48 hours after subculture) cells were trypsinized and seeded into the Matrigel invasion chambers as described above. Cells were allowed invade for another 48 hours and then were processed for colorimetric assay as described above in cell migration/invasion assay.

miRNA Mimic Transfections Experiment

HCT116 parental cells were seeded in 100 mm^2 Petri dishes at 1.5×10^6. The next day cells were transfected with specific miRNAs (miR-181d, miR-182-3p and miR-203) or scrambled miRNA control at the concentrations of 75 nM (SwitchGear Genomics, Menlo Park, CA) using DharmaFect Duo transfection reagent (GE Healthcare Dharmacon, Inc., Lafayette, CO) according to manufacturer's instructions. The miRNA mimics sequences are listed in Supplementary Table 2. Forty-eight hours later, conditioned media was collected for KLK6 ELISA and cells were processes for Western blot analysis and migration/invasion assays as described above. For each miRNA mimic, migration and invasion assays were done in sextuplet and repeated twice.

3′UTR Luciferase Reporters with miRNA Mimic Analysis

HCT116 parental cells were plated in 24-well plates at 0.12×10^6 cells per well and transfected with 300 ng/µl per well of GoClone 3′ UTR reporter constructs (PAM 3′ UTR, FOS 3′ UTR and EHF 3′ UTR (SwitchGear Genomics, Menlo Park, CA) and 50 nM of miRNA mimics (miR-181-d and miR-182-3p) or non-targeting miRNA controls using DharmaFect Duo transfection reagent, according to the manufacturers' instructions. The following controls were used: control plasmid encoding the 3′UTR sequence of the housekeeping gene glyceraldehyde 3′-phosphate dehydrogenase (GAPDH) and the Random 3′UTR plasmid, containing non-conserved, non-genic and non-repetitive human genomic fragments. Twenty-four hours after transfection, plates were removed from incubator, rinsed once with PBS and analyzed using the manufacturers' recommended protocol (LightSwitch Assay, SwitchGear Genomics). Luminescence signal was detected using a luminometer (Synergy 2 Multi-Detection Microplate Reader (Bio-Tek Instruments, Inc., Winooski, VT). Each experiment included transfections of miRNA mimics and control plasmid in triplicates.

Normalization was done according to the manufacturers' recommendations below: http://switchgeargenomics.com/sites/default/files/pdf/LightSwitch_3UTRnorm.pdf. Statistical analysis was done in each experiment independently.

Orthotopic Colon Cancer Model

In vivo experiments were conducted on 6 to 7 weeks old Severe Combined Immunodeficient (SCID) mice (CB-17/IcrACCscid, which were originally purchased from Taconic Inc. (Germantown, NY). The SCID mouse colony is housed at animal facility in the University of Arizona Cancer Center. The facility is AAALAC accredited, and holds an Animal Welfare Assurance # with the Public Health (File#A-3248-01). Mouse colonies were maintained under microisolation and were handled and manipulated only in laminar flow hoods. All procedures involving animals were conducted according to the University of Arizona Animal care and Use Committee policies.

For the animal survival study, Control clone 1 and shKLK6 clone 3 clonal cells were injected at the concentration of 2×10^6 cells in 50 µl of saline solution into the cecum between the mucosa and the muscularis externa layers of the cecal wall of anesthetized mice (15 animals per experimental group) by using a 30-gauge needle. Animals were observed twice weekly for adverse signs associated with tumor growth (e.g., >20% body weight loss, immobility, loss of grooming), at which time mice were euthanized. Metastatic colonization and tumors formed were counted postmortem.

Statistics

Statistical analysis of cell culture experimental data was performed using paired *t*-test or ANOVA (Microsoft Excel, Microsoft Corp.). Statistical analyses comparing rates of tumor formation between the groups were determined using two-way ANOVA followed by Bonferroni tests. The Kaplan–Meier curve for survival was estimated by groups. The long-rank test was employed to test the difference in the survival curves. Fisher's Exact test was employed to test the difference in incidence of metastases between genotype groups.

Results

Knockdown of KLK6 in HCT116 Cells

To investigate the significance of *KLK6* expression in metastatic colorectal cancer, we developed isogenic cell lines of HCT116 colon cancer cells with stable knockdown of *KLK6* expression using the commercially available KLK6 silencing plasmids (Supplementary Figure 1*A*) as described in Materials and Methods. To confirm efficiency of knockdown of *KLK6*, we first examined mRNA levels in bulk transfections of HCT116 cells with negative control plasmid and shKLK6 plasmids 1 to 4 using quantitative real-time PCR (qRT-PCR). We found that *KLK6* transcript levels in cells treated with shKLK6 plasmids 2 to 4, but not shKLK6 1, were significantly

lower compared to negative control plasmid (*$P < .01$, ***$P < .0004$ and **$P < .002$, respectively) (Supplemental Figure 1*B*). Because the shKLK6 plasmid 3 (shKLK6-3) produced the most significant inhibition of KLK6 transcript, we isolated individual clones from this cell line as well as from HCT116 cells transfected with negative control plasmid. Clonally selected negative control clones (Control clones 1 and 3) and shKLK6-3 clones (named as shKLK6 clones 1, 2, and 3) were evaluated further for expression of KLK6 at the level of transcription and protein secretion. At 48 hours after subculture, *KLK6* transcript levels in shKLK6 clone 2 and clone 3 were suppressed by 80% compared to Control clones 1 and 3 (Figure 1*A*, **$P < .02$), while shKLK6 clone 1 showed approximately a 50% reduction (*$P = .05$). The suppression of KLK6 expression in shKLK6 clone 2 and shKLK6 clone 3 was efficient and prolong since even at 7 days after subculture the levels of KLK6 in conditioned media from these shKLK6 clones remained significantly low (Figure 1*B*, *$P \leq .05$, **$P < .02$). A significant decrease of the KLK6 intracellular levels in shKLK6 clones 2 and 3 compared to HCT116 parental cell line and Control clone 1 corroborated with the decrease in KLK6 transcription in shKLK6 clones (Figure 1*C*). These data validated silencing of endogenous *KLK6* transcript in HCT116 cells isogenic clones expressing the shKLK6-3 plasmid.

Effect of KLK6 Knockdown on HCT116 Cell Growth, Migration and Invasion In Vitro

We assessed the growth of Control clone 1 and shKLK6 clones 1 to 3 by counting viable cells at different days after subculture using the trypan blue exclusion method. The statistically significant growth inhibition was noted for shKLK6 clone 2 on Days 4 and 6 after subculture but this clone grew comparable to others at later times (Supplementary Figure 2). Next, we evaluated the effect of *KLK6* knockdown on cell migration and invasion using Boyden migration/invasion chambers with the basement membrane-like substrate Matrigel. Cells were seeded either on control or Matrigel-coated inserts and allowed to migrate/invade for 48 hours. The migratory and invasive abilities were both suppressed in tested shKLK6 clone 2 and shKLK6 clone 3 compared to Control clone1 and Control clone 3 which expressed and secreted significant levels of KLK6 (Figure 2*A*. Migration through control inserts, *$P < .05$ and Figure 2*B*. Invasion through Matrigel- coated inserts, **$P \leq .03$). To confirm that KLK6 expression rescued the invasive phenotype of HCT116 cells, we re-expressed the full-length KLK6 plasmid (pcDNA3.1 KLK6) in shKLK6 clone 3 cells. The shKLK6 clone 3-transfected cells were seeded on Matrigel-coated inserts and allowed to invade for 48 hours. We observed a significant increase in the invasiveness of shKLK6 clone 3 cells transfected with pcDNA3.1 KLK6 plasmid, compared to mock-transfected shKLK6 cells (Figure 2*C*). Further, we measured the levels of KLK6 protein secreted into the conditioned media by the mock-transfected or KLK6-transfected shKLK6 clone 3 cells seeded on Matrigel. The shKLK6 clone 3 transfected with pcDNA3.1 KLK6 plasmid secreted 10-fold more KLK6 than the mock transfected cells (Figure 2*D*). These results confirmed that KLK6 expression and secretion is necessary to restore the invasive phenotype of HCT116 cells.

Effect of KLK6 Knockdown in an Orthotopic Colon Cancer Mouse Model

The Control clone 1 and shKLK6 clone 3 were selected for testing the consequences of KLK6 knockdown in vivo. Cells were injected into the cecum of SCID mice, and animal survival rates, as well as the presence and location of metastases were assessed, when animals were sacrificed. The duration of this experiment was 125 days. Animals in Control clone 1 group were becoming morbid earlier during the course of the experiment and the majority of them had to be sacrificed before the shKLK6-injected group (median survival time of Control clone 1 group was half of shKLK6 clone 3 group, as shown by Kaplan- Meier survival curve, Figure 3*A*, $P = .0005$). Since KLK6 is a secreted protein and can be detected in CRC patients [17], we measured KLK6 levels in the serum of tumor-bearing animals at days 10 through 35 after cell injection with 7 to 10 days interval between samples collection (samples were collected retro-orbitally). Animals

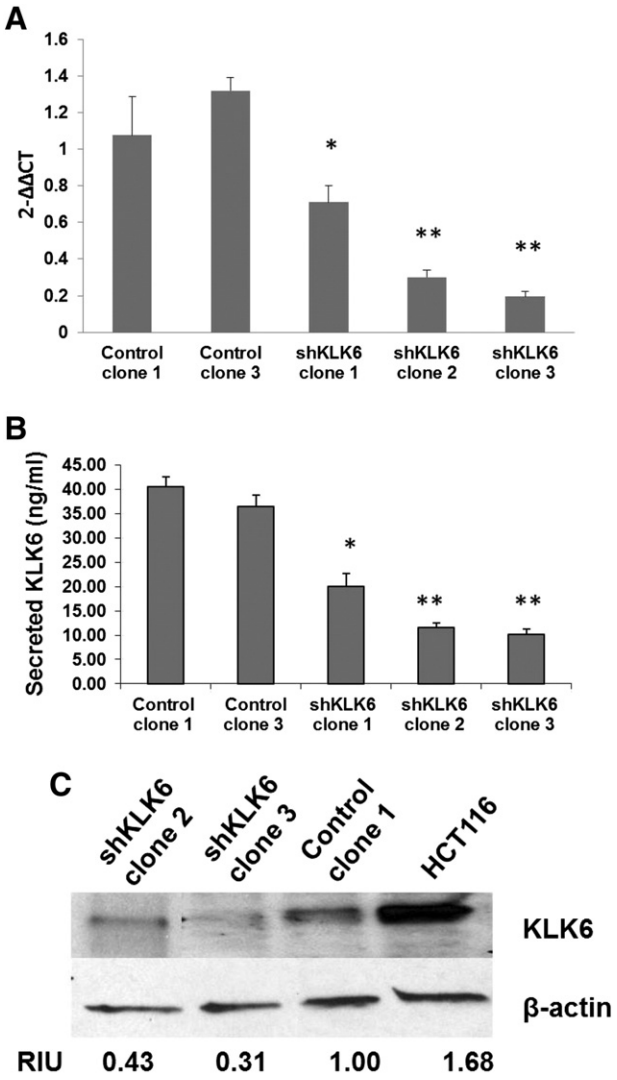

Figure 1. Validation of *KLK6* knockdown in HCT116 isogenic stable cell lines. (A) qRT-PCR for *KLK6* RNA levels in Control clones 1 and 3 and shKLK6 clones 1, 2, and 3 harvested 48 h after subculture. (B) Levels of secreted KLK6 in conditioned media at 7 days after subculture in Control clones 1 and 3 and shKLK6 clones 1, 2, and 3. *$P \leq .05$, Control clones vs. shKLK6 clone 1; **$P < .02$ Control Clones vs. shKLK6 clones 2 and 3 by ANOVA. (C) Intracellular levels of KLK6 in shKLK6 clones 2 and 3 as well as in Control clone 1 and HCT116 parental cells by Western blot analysis. Densitometry analysis was performed as described in "Materials and methods" section. Relative Intensity Units (RIU), which were calculated as protein/β-actin ratio normalized to Control Clone 1 sample).

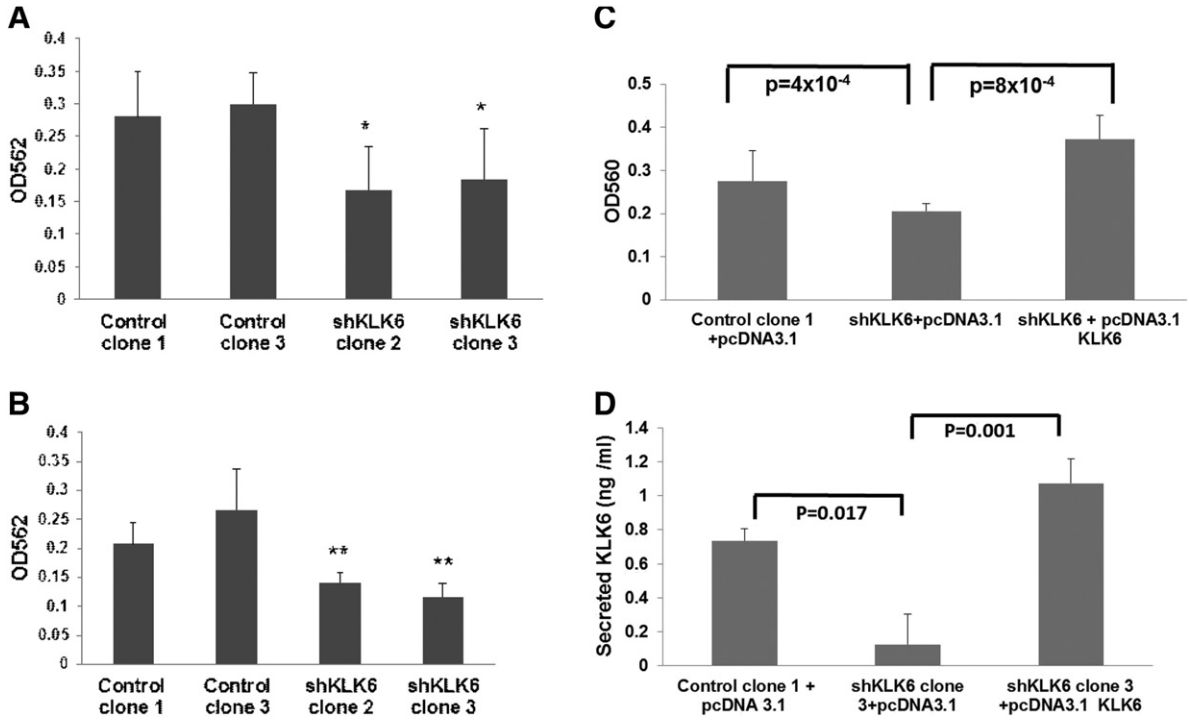

Figure 2. Suppression of KLK6 expression decreases cell migration and invasion. (A) Boyden chambers migration assay of Control clones 1 and 3 and shKLK6 clones 2 and 3, $*P < .05$. (B) Matrigel invasion assay of Control clones 1 and 3 and shKLK6–3 clones 2 and 3, $**P < .03$ by ANOVA. Figures are representative of three independent experiments. (C) Transient re-expression of KLK6 in shKLK6 clone 3 rescues invasive phenotype. Matrigel invasion assay of Control clone 1 and shKLK6 clone 3 transfected with either empty plasmid (pcDNA3.1) or plasmid expressing the full length KLK6 cDNA (pcDNA3.1 KLK6). Control Clone 1 and shKLK6 clone 3 were transiently transfections with indicated plasmids and 24 h later cells were trypsinized, re-seeded into Matrigel-covered Boyden chambers and allowed to invade for the 48 h. Analysis was done as described in "Materials and methods" section. Figure is representative of two independent experiments. In each experiment transfections were done in triplicate following by invasion assays in sextuplet. (D) Levels of KLK6 by ELISA in conditional media cells seeded in Boyden chambers 48 h after re-seeding. *P* values by *t*-test are indicated in the Figure.

injected with shKLK6 clone 3 had significantly lower levels of KLK6 in the serum compared to animals injected with Control clone 1 cells (Figure 3*B*, $P < .01$). Upon sacrifice, no difference was found in the primary tumor weights between animals injected with Control clone 1 and shKLK6 clone 3 (average weight 0.46 ± 0.36 vs. 0.57 ± 0.24, respectively). At the same time, the analysis of the severity of metastatic disease showed that animals injected with Control clone 1 developed significant number of metastases in the abdominal wall, mesentery, diaphragm, and liver, showing the similar pattern of dissemination as observed in CRC cancer patients. In contrast, shKLK6 clone 3 injected animals developed less metastasis to the diaphragm and mesentery wall (Table 1, $*P = .0068$ and $**P = .0373$, respectively). No macroscopically visible metastasis was detected in the abdominal wall of shKLK6 clone 3-injected animals, although this difference did not reach statistical significance due to variability among injected animals. The tumor spreading to the colon, which is near the primary site of injection (cecum), was comparable in shKLK6 clone 3 and HCT116 control clone 1 injected animals (Table 1). Taken together, these data suggest that KLK6 mediates distant colon cancer metastasis.

Identification and Correlation of miRNAs and mRNAs Differentially Expressed in KLK6 Knockdown Cells

Since in vitro and in vivo analyses both suggest the direct role of KLK6 in invasion and metastasis, we sought to identify genes and miRNAs involved in *KLK6*-mediated colon cancer metastasis formation. We hypothesized that a subset of genes may regulate the metastasis in the presence of the elevated *KLK6* level in colon cancer cells. To test this hypothesis, we performed concomitant miRNA and mRNA expression profiling of HCT116 control clone 1 and shKLK6 clone 3 using the Affymetrix Human Gene 1.0 ST (28,869 well-annotated genes) and Affymetrix GeneChip miRNA 2.0 arrays (1105 human mature miRNAs), respectively.

Gene Expression Results. More than 300 genes were found to be significantly altered in KLK6 knockout cells when compared to Control clone 1 cells. We focused on top 50 genes that were changing significantly based on the adjusted *P* value as shown in Table 2 and depicted in Supplemental Figure 3*A*. In this set, 36 gene transcripts were significantly down-regulated and 14 were up-regulated.

miRNA Expression Results

Based on the statistical analysis we found 30 miRNAs altered in KLK6 knockout cells compared to Control clone 1 cells (Table 3). Among the differentially expressed miRNAs, 21 were significantly down-regulated and nine were up-regulated (Supplemental Figure 3*B*).

Correlation of miRNAs and Their Targeted mRNAs. Probes with significant expression changes from mRNA and miRNA array experiments were analyzed further to detect miRNA-mRNA target pairs and their inverse correlation. Multiple methods were used to detect the mRNA and miRNA target pairs. Bioconductor package Rmir was used to search TargetScan and pictar databases for the differential expressed mRNA and miRNA. Further predicted human

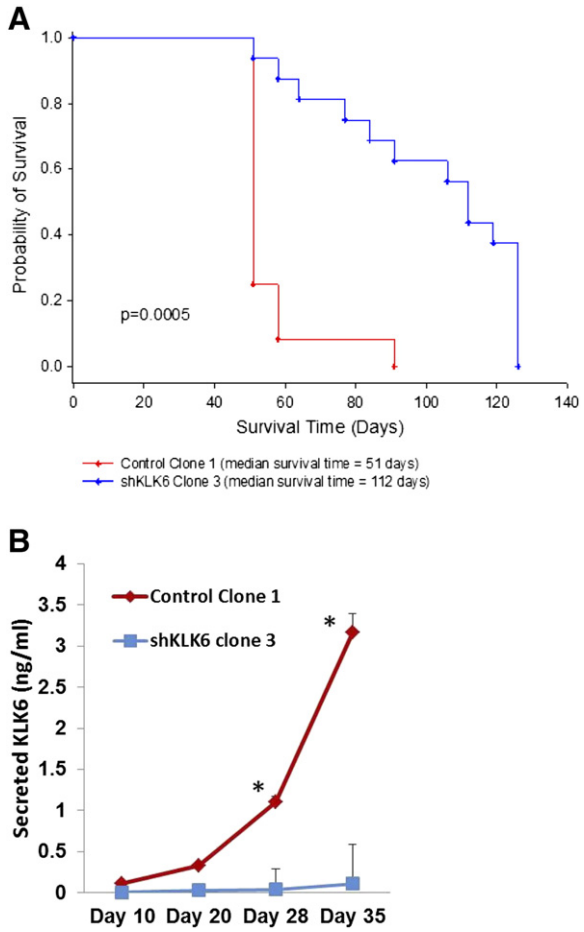

Figure 3. Testing the consequences of KLK6 knockdown in colon cancer cell in vivo. (A) Kaplan–Meier survival curve of SCID mice injected with Control clone 1 and shKLK6 clone 3 orthotopically (n = 15 mice per group; $P = .0005$ by long-rank test). (B) KLK6 levels by ELISA in the bloodstream of the tumor bearing animals, $^*P < .01$.

target mRNAs and miRNAs were extracted from TargetScan 5.2 [4] and microRNA.org (version 8-2010) [27]. The microRNA.org resource comprises predictions computed by the mirSVR-miRanda algorithm [28]. The only predictions that were considered, were those annotated as 'conserved miRNA' and 'good mirSVR score'. For the analysis, the intersection between microRNA.org and TargetScan predictions were taken into account. The applied bioinformatics tools identified six of the most significantly altered miRNAs and 37 gene transcripts targeted by those miRNAs (Figure 4*A*).

Table 1. The incidence of metastases in HCT116 control clone 1 (n = 15 mice) and shKLK6–3 clone 3 (n = 15 mice)

Location	Control clone 1	shKLK6 Clone 3
Liver	53.33%	18.75%
Diaphragm	40.00%	0.00% *
Mesentery	40.00%	6.25% **
Colon	13.33%	12.50%
Abdominal wall	26.67%	0.00%

* $P = .0068$.
** $P = .0373$ by Fisher's exact test.

Experimental Validation of Bioinformatic Predictions

From the set of six altered miRNAs described above, we selected three the most significantly altered microRNAs, miR-181d, miR-182 and miR-203, to further validate and explore their selected targeted genes. We confirmed that miR-181d was significantly down-regulated and miR-182, and miR-203 were significantly up-regulated ($^*P < .0001$) (Figure 4*B*). The genes predicted to be targeted by these miRNAs were identified using bioinformatics resources, such as microRNA.org and TargetScan.org, and are depicted in Figure 4*C*. The sequence alignments of selected miRNAs with the 3′UTR region of candidate target genes based on TargetScan.org search results are shown in Supplementary Figure 4*A*. The miR-181d is predicted to target the 3′UTR of *FBJ murine osteosarcoma viral oncogene homolog (FOS)*, *peptidylglycine alpha-amidating monooxygenase (PAM)*, and chondroitin sulfate proteoglycan *versican* (*VCAN),* at single locations, and *Ets Homologous Factor (EHF*) mRNA at two locations. For miR-182, predicted targets are 3′UTRs of *EHF* at one location, and *TGFβ2* at two locations. The putative sites of miR-203 targeting were identified in 3′UTRs of *Ric-related gene expressed throughout the organism* (*RIT1*), *transforming growth factor beta 2* (*TGF-β2)* (all at single locations) and the *Runt-related transcription factor 2 (RUNX2)* 3′UTRs at two locations. The relative positions of the predicted seed sequences in 3′UTRs of target genes are depicted in Supplementary Figure 4*B*. The supplementary Figure 4*B* implies that one gene can be regulated by multiple miRNAs, which can produce either co-operative or counteractive effects on expression of the targeted genes. We further validated the alterations of selected transcripts in shKLK6 clone 3 by qPCR (Figure 4*D*). Table 4 summarizes the validated altered miRNA-mRNAs sets and their cellular functions.

Functional Validation of Selected miRNA-mRNA Interactions

a. *Validation of predicted microRNA- targeted genes using 3′UTR reporter constructs*. Co-transfection of miRNA mimics (Switchgear Genomics, Inc.) and commercially available 3′UTR luciferase reporter plasmids (Switchgear Genomics, Inc.) was done in the HCT116 parental cell line. The GoClone reporter plasmids carrying the full length 3′UTR sequences of EHF, FOS or PAM mRNAs were co-transfected with miR-181d and miR-182 mimics into HCT116 cells and luciferase activity was measured 24 h later. The negative control plasmid encoding the 3′UTR of the glyceraldehyde 3′-phosphate dehydrogenase (GAPDH) sequence was used to normalize the luminescence values. The results showed a significant decrease in luciferase activity of the tested 3′UTRs that confirms the bioinformatics results that miR-181d can target the EHF, FOS and PAM 3"UTRs and miR-182-3p can interact with the 3′UTR of EHF (Figure 5*A*). However, the two putative miR-181d binding sites found in silico within the EHF 3′UTR (Supplementary Figure 4*B*) suggests that further assays need to be performed to determine which or if both predicted sites are targeted.

b. *Validation of selected miRNA-targeted proteins by Western blotting*. We measured levels of the selected proteins predicted to be targeted by miRNAs-181d, –182 and –203 after treatment with their respective miRNA mimics. We confirmed the altered expression (on average two-fold decrease in expression levels) of the following targeted proteins: FOS and VCAN, which are predicted to be targeted by miR-181d (Figure 5*B*, left panel); TGF-β2, RIT1, VCAN, RUNX2, which are predicted to be targeted by miR-203 (Figure 5*B*, right

Table 2. Top 50 significantly altered genes and their Log-Fold changes (LogFC) in HCT116 cells with knockdown of KLK6 expression

Gene Symbol	Description	EntrezID	logFC	*P*	adj. *P*
FOS	FBJ murine osteosarcoma viral oncogene homolog	2353	2.03	0.00000227	0.005505977
CEMIP	cell migration inducing protein, hyaluronan binding	57214	1.76	0.0000000632	0.001052012
ANGPT2	angiopoietin 2	285	1.57	0.0000000201	0.00067041
TNFRSF10D	tumor necrosis factor receptor superfamily, member 10d, decoy with truncated death domain	8793	1.07	0.000000177	0.001476945
RND3	Rho family GTPase 3	390	1.06	0.000000848	0.004031475
TPRG1	tumor protein p63 regulated 1	285386	0.95	0.0000074	0.006844187
CHN1	chimerin (chimaerin) 1	1123	0.85	0.00000209	0.005505977
ARRDC4	arrestin domain containing 4	91947	0.82	0.00000984	0.007424321
PXDN	peroxidasin homolog (Drosophila)	7837	0.76	0.0000118	0.008216496
TWF2	twinfilin, actin-binding protein, homolog 2 (Drosophila)	11344	0.71	0.0000204	0.010903194
ANO4	anoctamin 4	121601	0.70	0.00000528	0.006786285
PAM	peptidylglycine alpha-amidating monooxygenase	5066	0.65	0.0000206	0.010903194
PDE4B	phosphodiesterase 4B, cAMP-specific	5142	0.61	0.0000268	0.013225005
BAMBI	BMP and activin membrane-bound inhibitor homolog (*Xenopus laevis*)	25805	0.50	0.0000319	0.014760228
NUP62CL	nucleoporin 62 kDa C-terminal like	54830	-0.51	0.0000344	0.014822306
BRWD3	bromodomain and WD repeat domain containing 3	254065	-0.54	0.0000337	0.014822306
ANKIB1	ankyrin repeat and IBR domain containing 1	54467	-0.54	0.0000333	0.014822306
LOC554202	hypothetical LOC554202	554202	-0.59	0.00001	0.007424321
CASP4	caspase 4, apoptosis-related cysteine peptidase	837	-0.62	0.00000771	0.006859067
CCNE2	cyclin E2	9134	-0.65	0.0000125	0.008330166
TGFB2	transforming growth factor, beta 2	7042	-0.69	0.0000274	0.013225005
INPP4B	inositol polyphosphate-4- phosphatase, type II, 105 kDa	8821	-0.69	0.00000783	0.006859067
ARL4C	ADP-ribosylation factor-like 4C	10123	-0.70	0.0000192	0.010611066
CALB2	calbindin 2	794	-0.71	0.0000124	0.008330166
TRHDE	thyrotropin-releasing hormone degrading enzyme	29953	-0.71	0.0000347	0.014822306
C17orf60	chromosome 17 open reading frame 60	284021	-0.72	0.0000259	0.013041394
ARFGAP3	ADP-ribosylation factor GTPase activating protein 3	26286	-0.75	0.00000558	0.006786285
RIT1	Ras-like without CAAX 1	6016	-0.75	0.0000148	0.009274971
ANKRD36	ankyrin repeat domain 36	375248	-0.80	0.0000256	0.013041394
EHF	*Ets* homologous factor	26298	-0.81	0.00000955	0.007414408
FLJ41309	hypothetical LOC645079	645079	-0.82	0.00000713	0.006786285
CNTNAP3	contactin associated protein-like 3	79937	-0.82	0.00000272	0.005665154
ANKRD36B	ankyrin repeat domain 36B	57730	-0.83	0.00000687	0.006786285
RUNX2	runt-related transcription factor 2	860	-0.87	0.0000172	0.009715138
FLJ36840	hypothetical LOC645524	645524	-0.87	0.00000153	0.005505977
TLR3	toll-like receptor 3	7098	-0.88	0.00000166	0.005505977
MNS1	meiosis-specific nuclear structural 1	55329	-0.93	0.00000958	0.007414408
PRSS12	protease, serine, 12 (neurotrypsin, motopsin)	8492	-0.95	0.00000197	0.005505977
PRO2012	hypothetical protein PRO2012	55478	-0.98	0.00000403	0.006661463
VCAN	versican	1462	-0.99	0.00000548	0.006786285
SEMA3D	sema domain, immunoglobulin domain (Ig), short basic domain, secreted, (semaphorin) 3D	223117	-1.01	0.000017	0.009715138
APOBEC3G	apolipoprotein B mRNA editing enzyme, catalytic polypeptide-like 3G	60489	-1.03	0.00000366	0.006407034
TCN1	transcobalamin I (vitamin B12 binding protein, R binder family)	6947	-1.06	0.0000271	0.013225005
CYP24A1	cytochrome P450, family 24, subfamily A, polypeptide 1	1591	-1.07	0.000000474	0.002630928
SYTL2	synaptotagmin-like 2	54843	-1.09	0.00000243	0.005505977
NRP1	neuropilin 1	8829	-1.09	0.00000161	0.005505977
GNG11	guanine nucleotide binding protein (G protein), gamma 11	2791	-1.12	0.0000164	0.009715138
GLIS3	GLIS family zinc finger 3	169792	-1.14	0.0000035	0.006407034
DPP4	dipeptidyl-peptidase 4	1803	-1.28	0.0000154	0.009477414
KLK6	kallikrein-related peptidase 6	5653	-1.74	0.000000161	0.001476945

panel). Although in silico analysis did not find any binding sites for miR-182 in the 3′UTR of VCAN mRNA, the level of VCAN protein was found to be suppressed by miR-182-3p mimic (Figure 5*B*). At the same time, the level of TGF-β2 protein, which is predicted to be targeted by miR-182, was found to be elevated. These observations reflect the complexity of interactions among miRNAs and their predicted targets and may be explained by changes in ratios of different miRNAs available for binding to the target mRNAs at the specific time.

Because the TGF-β signaling pathway is one of the major signaling pathways inducing the EMT in cancer [29] and TGF-β2 was identified as a putative target of miR-203, we explored further the effect of miR-203 on TGF-β-mediated EMT. We measured the TGF-β2 protein level in HCT116 cells upon transfection with miR-203 mimic and observed miR-203-dependent suppression of the TGF-β2 protein level (~1.8-fold decrease on average) (Figure 5*C*). The other two proteins tested were transcription factors involved in the EMT program: Snail1 (also known as Snail) and the high-mobility group AT-hook 2 (HMGA2). Snail is the major transcription factor downstream of TGF-β that controls expression of other epithelial molecules, such as claudins, occludins, and mucin 1 and suppresses them during transition to the mesenchymal and invasive phenotype [30]. To demonstrate that the TGF-β signaling is intact in HCT116 cells we treated cells with TGF-β2 ligand, and showed more than 2-fold induction of Snail protein, which was reversed by miR-203 mimic (Figure 5*C*). MiR-203 has been reported to regulate the expression of Snail through two binding sites within its 3′UTR and also controls Snail expression via a specific double negative miR-203/Snail RNA feedback loop [31]. The transcription factor HMGA2 is also implicated in the EMT program, acting through the TGF-β signaling pathway [32,33]. We found that miR-203 treatment caused the significant 2.9-fold suppression of HMGA2 protein level. Bioinformatics analysis did not predict any

Table 3. Top 30 altered miRNA and their associated log-fold changes (LogFC)

miRNA Symbol	Mean_HCT116_control	Mean_shKLK6	LogFC	*P*
hsa-mir-718	5.294947654	6.754036124	1.45908847	0.045879181
hsa-mir-203	7.029301149	8.020819799	0.99151865	0.008956982
hsa-mir-182	10.29352168	11.15478097	0.861259299	0.015434767
hsa-mir-548 h-4	2.884592843	3.622983972	0.73839113	0.049694134
hsa-mir-183	7.582421649	8.317062777	0.734641128	0.008237583
hsa-mir-3118-1	2.686656791	3.141930151	0.45527336	0.039966262
hsa-mir-3118-2	2.686656791	3.141930151	0.45527336	0.039966262
hsa-mir-3118-3	2.686656791	3.141930151	0.45527336	0.039966262
hsa-mir-1278	3.244551972	3.6993644	0.454812428	0.032830919
hsa-mir-648	5.527078224	5.085925032	-0.441153192	0.038101421
hsa-mir-548f-3	3.327951758	2.866221129	-0.46173063	0.045867792
hsa-mir-4270	9.329300958	8.843975171	-0.485325786	0.044746584
hsa-mir-1301	6.74505824	6.18688073	-0.55817751	0.04917569
hsa-mir-3116-2	4.051649554	3.411182752	-0.640466802	0.009766037
hsa-mir-1276	4.490115372	3.834323045	-0.655792327	0.051910054
hsa-mir-214	8.95404013	8.273956951	-0.680083179	0.027345777
hsa-mir-608	4.73429596	4.015324807	-0.718971153	0.033354443
hsa-mir-330	5.785958752	5.059805273	-0.726153479	0.034693607
hsa-mir-1208	5.024649786	4.275301036	-0.74934875	0.002634706
hsa-mir-181b-1	8.773021975	7.921179422	-0.851842553	0.026985615
hsa-mir-4277	3.988026543	3.029042193	-0.958984351	0.017739471
hsa-mir-181b-2	8.917382218	7.948311081	-0.969071138	0.016964084
hsa-mir-4294	5.720753672	4.745005492	-0.97574818	0.03354712
hsa-mir-3182	4.951427444	3.947285402	-1.004142042	0.03471959
hsa-mir-3163	5.574709523	4.545762998	-1.028946525	0.031174295
hsa-mir-1256	3.825993651	2.773575511	-1.052418141	0.039276028
hsa-mir-181d	8.103003726	6.894016758	-1.208986967	0.018335536
hsa-mir-3127	6.79589692	5.583243032	-1.212653888	0.05200504
hsa-mir-3161	5.188485579	3.915881448	-1.272604131	0.010378268

binding sites for miR-203 within the 3′UTR of HMGA2 mRNA; therefore, we attributed the observed suppression to the downstream signaling through TGF-β, which was previously reported [33]. The phase-contrast images of HCT116 cells treated with miR-203 mimic at concentration of 75 nM demonstrate that miR-203 promotes epithelial-like features in HCT116 cells pre-treated with TGF-β2 ligand (Supplementary Figure 5).

Transient Transfection of miR-181d or miR-203 Inhibits KLK6 Expression and Cell Invasion

The above validation of miRNA targets was done in HCT116 colon cancer cells which express significant amount of KLK6 endogenously [34]. Here we investigated how the level of endogenous KLK6 is modulated by the selected miRNAs identified in KLK6 knockdown cells. We measured the intracellular and secreted levels of KLK6 protein upon treatment with miR-181d, miR-182 and miR-203 mimics. We found that the 48-hour treatment with the individual miRNA mimics at the concentration of 75 nM caused the decrease of both the intracellular and secreted KLK6 levels (Figure 6*A* and *B* (*$P \leq .02$), respectively). The intracellular level of KLK6 protein was not affected when cells were pretreated with the TGF-β2 ligand alone, but increased slightly upon addition of miR-203, while the secreted KLK6 was significantly decreased in the presence of TGF-β2 ligand and miR-203 (**$P = .002$) suggesting that miR-203 may also inhibit KLK6 protein secretion. Next, we conducted Matrigel invasion assays with selected miRNAs and observed decrease in cell invasion after transfection with miR-181d and miR-203 mimics, but not the miR-182-3p mimic (Figure 6*C*, *$P \leq .002$). The HCT116 cells migration was inhibited after transfection with miR-203 mimic at two different concentrations (Supplementary Figure 6*C*), but miR-181d and miR-182 did not alter cell migration (data not shown). In silico analysis identified a poorly conserved

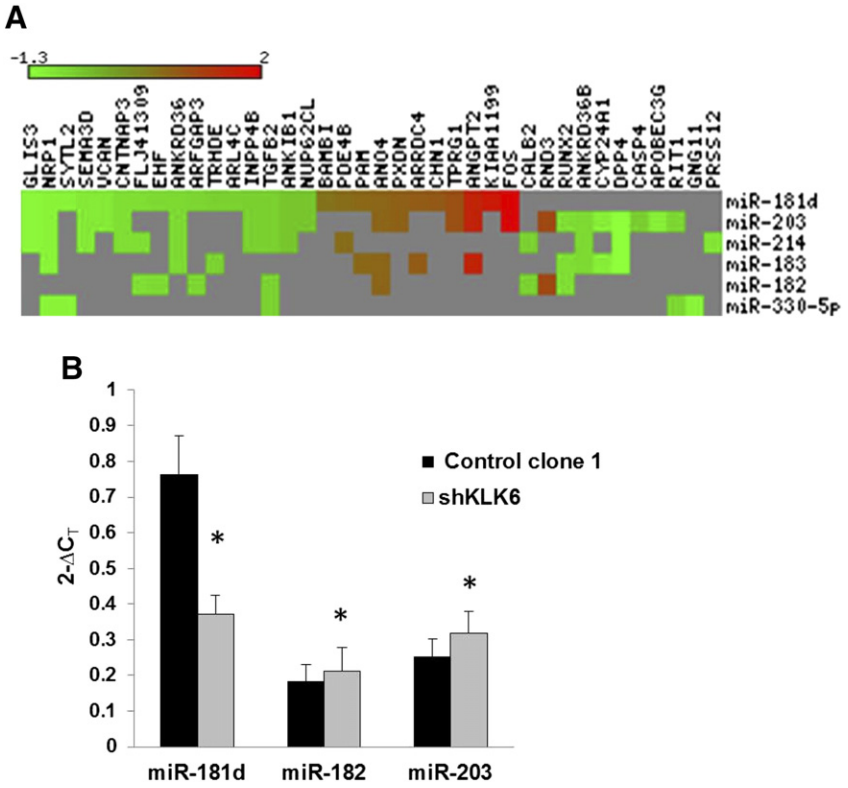

Figure 4. Validation of selected miRNAs and their predicted target genes by qRT-PCR. (A) Heat map of six miRNAs and their predicted targeted 37 genes. (B) Conformation of down-regulation of miR-181d and up-regulation of miR-182 and miR-203 in KLK6 knockdown cells. *$P < .0001$. (C) Relationship between validated altered miRNAs and their predicted target genes. (D) Conformation of altered expression of selected genes *$P \leq .05$, **$P \leq .02$, ***$P = .002$ by ANOVA.

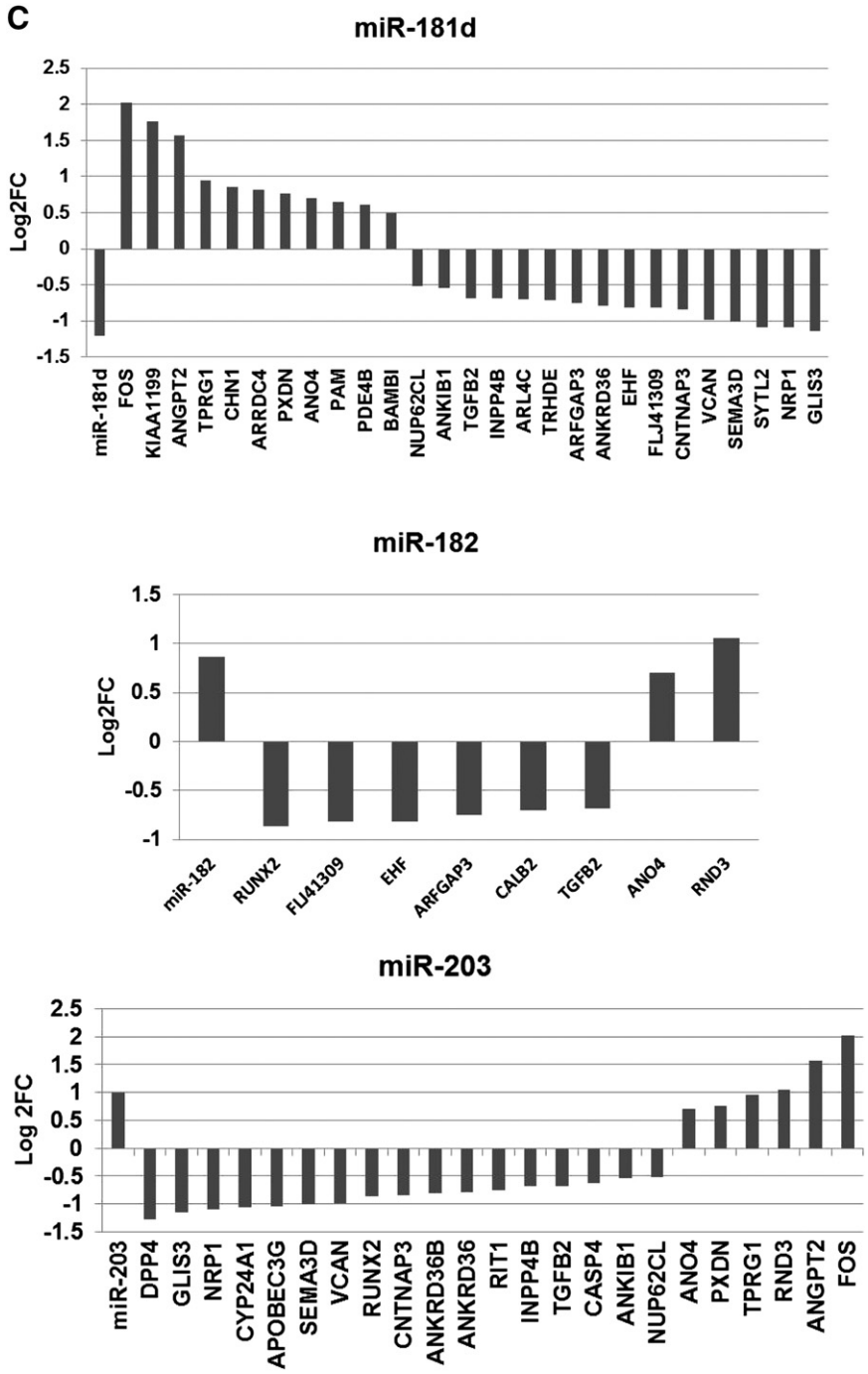

Figure 4. *(continued.)*

7-mer seed binding region for miR-203, but not miR-181d or miR-182 in the KLK6 3′UTR, (Supplementary Figure 6*A*). The ability of KLK6 3′ UTR to interact with miR-203 was tested in co-transfection experiment with the luciferase reporter vector carrying KLK6 3′UTR and miRNAs mimics. This functional analysis showed that miR-203, but not miR-181d and miR-182, is capable of binding to KLK6 3′UTR (Supplementary Figure 6*B*). Thus, decrease of the intracellular KLK6 protein in the presence of miR-181d and miR-182 mimics suggests rather indirect involvement of these miRNAs in KLK6 expression and secretion.

Discussion

We have previously shown that blocking of KLK6 expression in HCT116 cells by using small interference KLK6 RNA or KLK6-specific antibody decreased the ability of cells to migrate and invade though Matrigel [21]. The goal of the current study was to investigate the role and mechanism of KLK6-regulated cell invasion in colon cancer. To study KLK6 role in invasion we generated HCT116 isogenic cell lines with stable KLK6 knockdown (shKLK6 clones). Down-regulation of KLK6 in knockdown clones was confirmed at mRNA and protein levels (both expression and secretion). Further, we investigated the consequences of KLK6 inhibition on invasion in vitro, using the Matrigel invasion assay. Knockdown of KLK6 in colon cancer cells did not alter the cell growth, but suppressed the migration and invasion in vitro. Analysis of KLK6 knockdown in vivo was done using the SCID orthotopic colon cancer model. The animal study showed that the Control clone

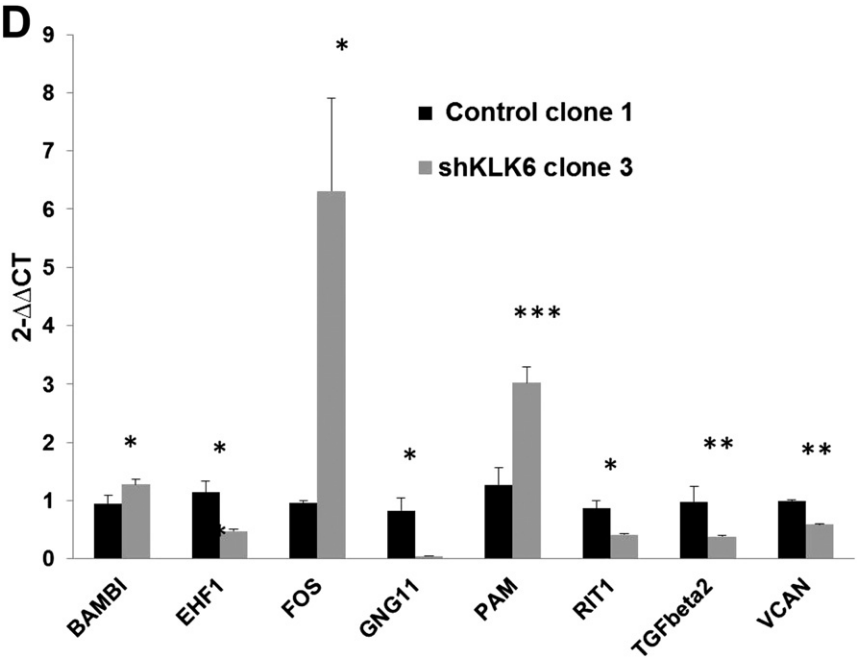

Figure 4. *(continued.)*

1 and shKLK6 clone 3-injected mice developed comparable colon tumors at the site of injection (cecum), but the shKLK6 tumors were not able to metastasize into distant organs (diaphragm and mesentery wall). As a result, the shKLK6-injected animals had doubled their survival rates, compared to the Control group (P = .005).

Metastasis is a complex process of interactions between transformed cells of the primary tumor, extracellular matrix components, blood and lymph vessels, and cells in the surrounding tissues, which provide growth factors and hormones. To understand the mechanism of KLK6-mediated metastatic progression in colon cancer we decided to focus on microRNAs, which have been linked to the different aspects of cancer pathology, including a metastatic disease [3,35,36]. MiRNAs regulate gene expression post-transcriptionally through binding to specific sites within the 3′UTR regions of targeted genes. Significant evidence collected in recent years demonstrates the essential role of mRNAs in the progression of colorectal cancer and suggests the use of miRNAs as possible CRC biomarkers [37]. In our study we applied Affymetrix mRNA and miRNA arrays to identify the miRNAs and their target genes which play an essential role in KLK6-driven cell invasion. Through bioinformatics analysis we initially selected a set of top six the most significantly altered miRNAs and 37 gene transcripts associated with the altered expression of KLK6. The miR-181d was found to be the most significantly suppressed miRNA in KLK6 knockdown cells (logFC −1.209, P = .0183). The miRNA-181d (Chr19p13.13) is located within the largest miRNA cluster of 43 miRNAs on chromosome 19. The most significantly up-regulated miRNAs in KLK6 knockdown cells were also identified: miRNA-182 (Chr7q32.2, logFC 0.861, P = .015) and miRNA-203 (Chr14q32.33, logFC 0.992, P = .009). All these miRNAs are transcribed from intergenic regions, where an individual miRNA gene or a cluster of miRNAs (in case of miR-181 and miR-182) form an independent transcriptional unit. We confirmed altered expression of miRNAs-181d, −182 and −203 and validated their effects on predicted target genes either by co-transfection of miRNA mimics with 3′UTR luciferase reporter constructs or by Western blot analysis of targeted proteins. Further, we evaluated the ability of these miRNAs to alter cell invasion and found that treatment with miR-181d and miR-203 mimics significantly suppressed HCT116 cells invasion through Matrigel.

The level of miR-181d was found to be suppressed in HCT116 cells upon KLK6 knockdown. We tested miR-181d status in another colon cancer cell line, Caco-2, which does not express KLK6 and does not form metastasis in vivo,and found that miR-181d level in this cell line was significantly higher than in HCT116 cells (data not shown).

Table 4. Summary of validated miRNAs and mRNAs and their metastasis-associated cellular functions

miRNA	Validated miRNA Expression	Predicted RNA Targets	Validated RNA Expression	Involvement in cellular process
miR-181d	Down	PAM	Up	*Peptidylglycin alpha-amidating monooxygenase.* Involve in posttranslational modification of bioactive proteins.
		BAMBI	Up	*BMP and activin membrane-bound inhibitor.* Involve in TGF-β signaling inhibition.
		FOS	Up	*FBJ murine osteosarcoma viral oncogene*. Nuclear phosphoprotein, regulator of cell proliferation, differentiation and transformation.
		VCAN	Down	*Versican.* Component of extracellular matrix, involve in cell adhesion, proliferation, migration.
miR-182	Up	EHF	Down	*ETS homologous factor.* Transcriptional activator of a subset of genes that control cell proliferation, transformation and apoptosis.
		TGF-β2	Down	*Transforming growth factor β2.* Secreted protein, regulates proliferation, differentiation, adhesion, migration via TGF-β-SMAD pathway.
miR-203	Up	RIT1	Down	*RAS-like without CAAX.* RAS-related GTPase, regulates p38 MAPK-dependent signaling.
		RUNX2	Down	*Runt-related transcription factor 2.* Essential for osteoblastic differentiation and skeletal morphogenesis.
		TGF-β2	Down	As above.
		VCAN	Down	As above.

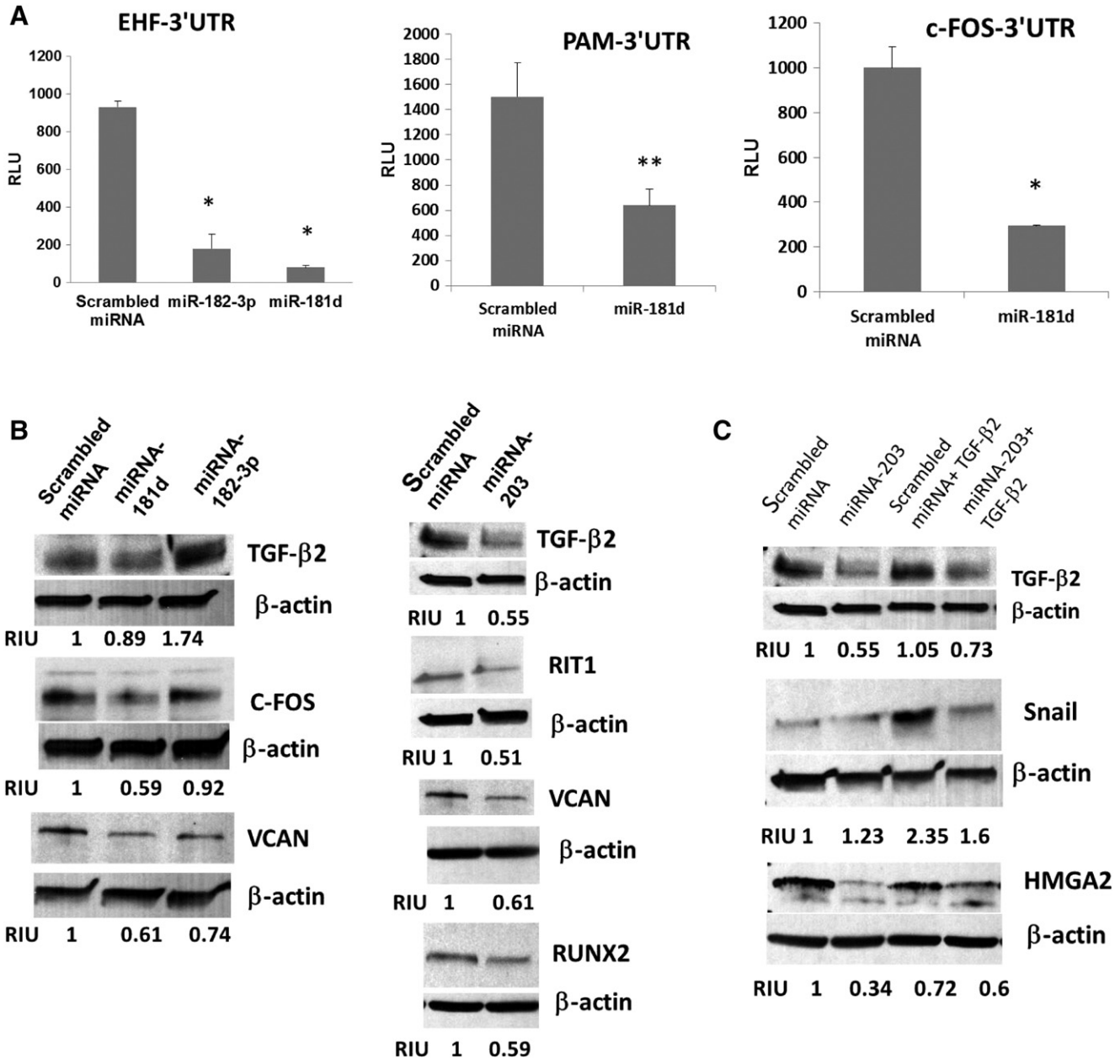

Figure 5. Validation of selected miRNA-mRNA interactions. (A) 3′UTR reporter assays confirming the interaction of miR-181d and miR-182-3p with the 3′UTR of their candidate target genes: EHF (EHF-3′UTR), PAM (PAM-3′UTR) and FOS (FOS-3′UTR). Luciferase assays were done 24 h after co-transfections of the 3′UTR luciferase constructs with miR-181d or miR-182-3p or scrambled miRNA at the concentration of 50 nM. RLU: Relative luciferase units, which were calculated as a ratio of 3′UTR activity of gene transcript transfected with selected miRNAs and average 3′UTR activity of control plasmids as described in Materials and Methods section. Each experiment was performed in triplicates and repeated twice $^{*}P < .003$, $^{**}P = .017$ by *t*-test. (B) Western blot analysis of selected proteins altered by treatment with miR-181d and miR-182 mimics. HCT116 cells were transfected with the scramble miRNA or each of selected miRNA mimics at the concentration of 75 nM and protein levels of their targeted genes (c- FOS, VCAN) were measured by Western blotting 48 h after transfection. (C) Treatment with miR-203 mimics alters the expression of proteins which regulates the EMT. HCT116 cells were transfected either with the scrambled miRNA control, miRNA-203 in the presence of absence of TGF-β ligand (5 ng/ml in a serum-free media). The intracellular level of the EMT marker Snail was measured to verify the TGF-β2–mediated EMT in HCT116 cells (Right panel). β-actin was used as a loading control. Protein bands quantitation was done using Image J software and presented as Relative Intensity Units (RIU), which were calculated as protein/β-actin ratio normalized to scrambled miRNA sample). Figures are representative of two independent experiments.

This observation suggests a regulatory feedback relationship between KLK6 and miR-181d in colon cancer cells. Similarly, the levels of miR-181d were found to be low in human glioma samples [38], as KLK6 has been reported to be elevated in patients with the advanced stages of glioma [39]. The ectopic expression of miR-181d in glioma cell lines lead to suppression of cell proliferation, cell cycle arrest and apoptosis [38]. Together these data indicate that miR-181d has a tumor-suppressive properties and may act through regulation of KLK6 expression. Previously done bioinformatics analysis predicted that members of miR-181 family, miR-181b-1, –2/c/d can target

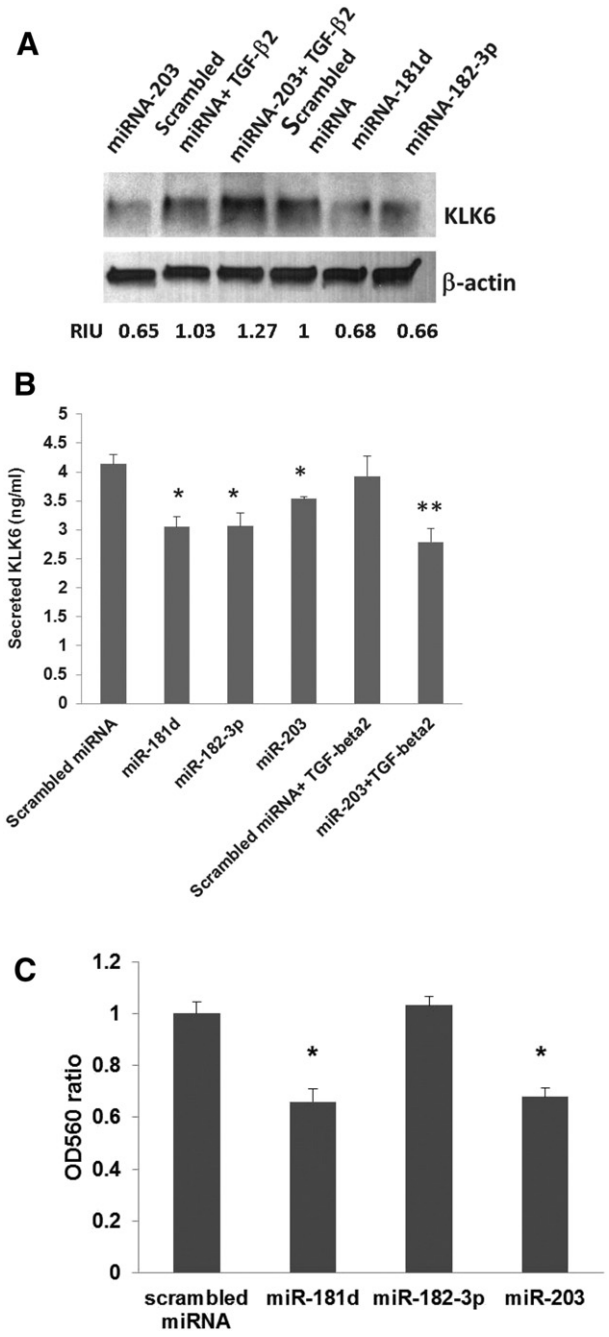

Figure 6. Effect of selected miRNA mimics on KLK6 expression and/or secretion and invasion in HCT116 colon cancer cells. (A) Western blot analysis of KLK6 intracellular protein level in HCT116 cells treated with miR-181d, miR-182 and miR-203 mimics. HCT116 cells were transfected with each of selected miRNA mimics at concentration of 75 nM and cells were processed for Western blot analysis 48 h after transfection. Some cell culture plates were also treated with TGF-β2 ligand (5 ng/ml in a serum-free media) and/or miR-203 mimic. β-actin was used as a loading control. Protein bands quantitation was done using Image J software and presented as Relative Intensity Units (RIU, protein/β-actin ratio normalized to scrambled miRNA sample). Figure is a representative of two independent experiments. (B) Concentration of KLK6 in the conditioned media of HCT116 cells upon treatment with selected miRNA mimics by ELISA $*P \leq .02$,$**P = .002$ by *t*-test. (C) Matrigel invasion assay of HCT116 cells treated with individual miRNA mimics. Cells were seeded onto Matrigel coated Boyden chambers 24 h after transfections and allow to invade for 48 hours. Analysis was done as described in Material and Methods section $*P \leq .002$ by *t*-test.

another member of serine proteinase family, KLK13, in breast and ovarian cancer; however, there have been no follow-up study to confirm this prediction [23]. Recent miRNA expression profiling study in a breast cancer cell line stably transfected with preproKLK5 revealed a 25.6-fold increase in miR-181c-5p level with a concomitant decrease of ten mRNA targets encoding extracellular matrix proteins [40]. Thus, the regulatory signaling, probably, exists between kallikreins and the members of miR-181 family of miRNAs.

Our results also point to a significant effect of miR-203 on migration and invasion of colon cancer cells. We show that this effect is due to the pivotal role of miR-203 in regulating the EMT through direct targeting of TGF-β2. TGF-β2 stimulates EMT during the early stages of the transition via up-regulation of Snail following the subsequent expression of ZEB1/2, Snail2 (also known as SLUG) and TWIST1 which maintain the mesenchymal phenotype [41,42]. The double-negative feedback loop involving TGFβ, ZEB and miR-200 family, which plays a significant role in the establishment and maintenance of EMT, has been previously identified in invasive ductal carcinomas and also is important for embryonic development and tumor metastasis [43,44]. Recent study in xenograft mouse model of head and neck squamous cell carcinoma showed that treatment with miR-203 mimic can inhibit lung metastasis through suppression of the pro-metastatic proteins involved in extracellular matrix remodeling, cell metabolism and cytoskeleton [45].

HCT116 cell line is a microsatellite unstable colorectal cancer line and has a truncating mutation in the type II TGF-β receptor. Nevertheless, HCT116 cells maintain their sensitivity to the TGF-β signaling, as we showed in the TGF-β2 ligand-treated cells, similar to other microsatellite unstable cell lines [46]. Treatment of HCT116 cells with miR-203 resulted in suppression of TGF-β2, Snail and HMGA2 proteins, which suggests the existence of miR-203-TGF-β2–HMGA2 signaling axis. The HMGA2 expression is implicated in the EMT program through the TGF-β signaling pathway [32] and is associated with a poor survival in colorectal cancer patients [47]. All three miRNA mimics inhibited the levels of intracellular and secreted KLK6 protein when they were introduced transiently, but only miR-181d and miR-203 mimics suppressed the invasion of HCT116 cells through Matrigel. Our bioinformatics analysis shows that miR-203, but not miR-181d or miR-182 could target the KLK6 3"UTR. The posttranscriptional regulation of KLKs through specific miRNAs has been previously suggested [23]. The most conserved predicted miRNAs for KLK6 3"UTR are the members of the let-7 family of miRNAs and none of them were altered in shKLK6 cells in significant manner.

There is a growing interest to understand the complex molecular networks regulated by kallikreins in cancer. Previously done bioinformatics analysis of miRNAs dysregulated in human prostate cancer identified the inverse interactions between 29 miRNAs and 10 members of KLK family with potential clinical applications [48]. The important link has been recently established between KLK6 and specific miRNAs expressed in the luminal and basal-like molecular subtypes of breast cancer that can predict the patients survival outcome [49]. Particularly, KLK6 overexpression in breast cancer cells induced miRNA biogenesis and correlated with the expression of genes involved in cell-cycle control (e.g., CDKN1B, cyclin D), MAPK, Wnt signaling pathways and EMT (e.g., miR-34a). The KLK6-regulated networks reported in breast cancer cells [49] and identified here in the colon cancer cells demonstrate that KLK6 regulates common signaling pathways in epithelial tumors, although

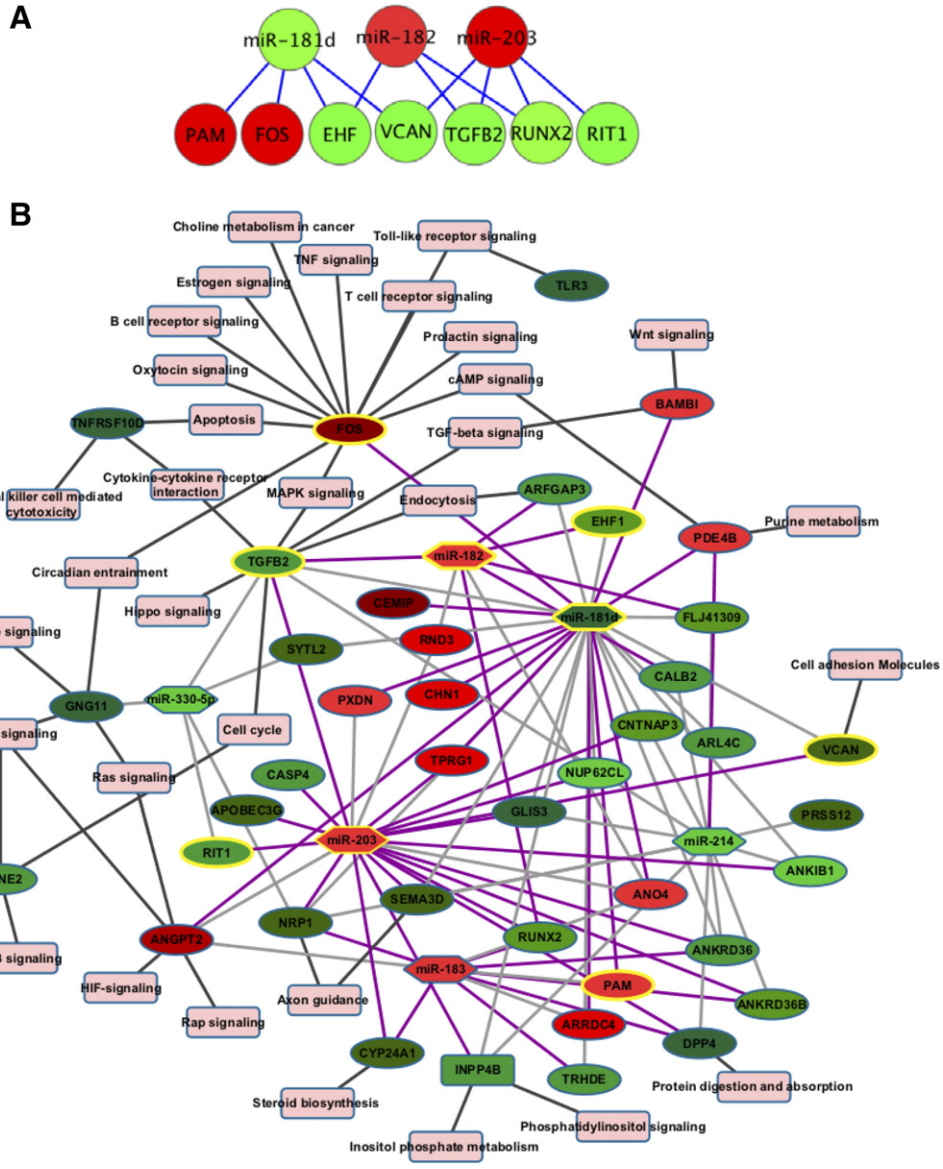

Figure 7. (A) Validated miRNA-mRNA network in HCT116 cells with knockdown of KLK6 gene. (B) Network of predicted miRNA-RNA target pairs and pathways for the gene targets. Cytoscape [52] was used to generate the network. Pink Nodes are Kegg pathways; Green colored nodes indicate decrease in expression; Red colored nodes indicate increase in expression. Dark gray edges show genes connected to pathways. Light gray edges show relationship between miRNAs and their target genes. Purple edges show inverse correlation between miRNAs and their target genes. Nodes with a yellow border are the three miRNAs and the six mRNAs for which inverse correlations have been confirmed experimentally.

the KLK6-mediated miRNA and mRNA targets within these pathways may differ due to the organ-specific expression and regulation.

In summary, our bioinformatics and experimental approaches provide the analysis of miRNA-miRNA networks regulated through KLK6 in colon cancer cells. In the present study, we profiled miRNAs and mRNAs in the colon cancer cells, which lost their invasive phenotype due to knockdown of expression of KLK6. We established and validated a network of two up-regulated miRNAs (miR-182, miR-203) and one down-regulated miRNA (miR-181d), that regulates expression of genes involved in proliferation, differentiation and post-translational modification (FOS, EHF, PAM), EMT (TGF-β2), RAS (RIT1) and invasion (RUNX2, VCAN) signaling pathways (Figure 7*A*).

We constructed a regulatory network of validated miRNA and mRNA which demonstrates the complexity of miRNAs interactions with their target genes in colon cancer cells expressing KLK6 (Figure 7*B*). Based on the predicted interactions, a few dysregulated miRNAs can have a significant effect on multiple signaling pathways, as has been postulated by Gurtan and Sharp [50]. The American Society of Clinical Oncology (ASCO) recommends the development and use of novel tumor marker with high specificity and sensitivity for the prevention, screening, treatment and surveillance of all gastrointestinal cancers and, particularly, colon cancer [51]. The miRNAs, identified in this study, present a promising targets for future anti-metastatic application.

Acknowledgements

We thank Dr. Georgrios Pampalakis and Dr. Georgia Sotiropoulou, Department of Pharmacy, University or Patras, Greece for providing us with a KLK6-expressing plasmid. We also would like to acknowledge the personnel of the University of Arizona Cancer

Center Experimental Mouse Shared Resource (EMSR) and Bioinformatics Shared Resource (GSR) at the University of Arizona Cancer Center for technical support in performing studies involving animals and miRNA microarray, respectively. We also thank Dr. Eleftherios P. Diamandis, Advanced Centre for Detection of Cancer, and members of his research group for providing the technical expertise in detecting of KLK6 in serum samples.

Appendix A. Supplementary Data

Supplementary data to this article can be found online at http://dx.doi.org/10.1016/j.neo.2017.02.003.

References

[1] Siegel RL, Miller KD, and Jemal A (2016). Cancer statistics, 2016. *CA Cancer J Clin* **66**, 7–30.
[2] Valastyan S and Weinberg RA (2011). Tumor metastasis: molecular insights and evolving paradigms. *Cell* **147**, 275–292.
[3] Fearon ER (2011). Molecular genetics of colorectal cancer. *Annu Rev Pathol* **6**, 479–507.
[4] Friedman RC, Farh KK, Burge CB, and Bartel DP (2009). Most mammalian mRNAs are conserved targets of microRNAs. *Genome Res* **19**, 92–105.
[5] Leung AK and Sharp PA (2006). Function and localization of microRNAs in mammalian cells. *Cold Spring Harb Symp Quant Biol* **71**, 29–38.
[6] Ebert MS and Sharp PA (2012). Roles for microRNAs in conferring robustness to biological processes. *Cell* **149**, 515–524.
[7] Esquela-Kerscher A and Slack FJ (2006). Oncomirs - microRNAs with a role in cancer. *Nat Rev Cancer* **6**, 259–269.
[8] Hammond SM (2006). MicroRNAs as oncogenes. *Curr Opin Genet Dev* **16**, 4–9.
[9] Lee YS and Dutta A (2006). MicroRNAs: small but potent oncogenes or tumor suppressors. *Curr Opin Investig Drugs* **7**, 560–564.
[10] Nazarov PV, Reinsbach SE, Muller A, Nicot N, Philippidou D, Vallar L, and Kreis S (2013). Interplay of microRNAs, transcription factors and target genes: linking dynamic expression changes to function. *Nucleic Acids Res* **41**, 2817–2831.
[11] Guo L, Zhao Y, Yang S, Zhang H, and Chen F (2014). Integrative analysis of miRNA-mRNA and miRNA-miRNA interactions. *Biomed Res Int* **2014**, 907420.
[12] Borgono CA and Diamandis EP (2004). The emerging roles of human tissue kallikreins in cancer. *Nat Rev Cancer* **4**, 876–890.
[13] Emami N and Diamandis EP (2007). Human tissue kallikreins: a road under construction. *Clin Chim Acta* **381**, 78–84.
[14] Paliouras M, Borgono C, and Diamandis EP (2007). Human tissue kallikreins: the cancer biomarker family. *Cancer Lett* **249**, 61–79.
[15] Sotiropoulou G, Pampalakis G, and Diamandis EP (2009). Functional roles of human kallikrein-related peptidases. *J Biol Chem* **284**, 32989–32994.
[16] Magklara A, Mellati AA, Wasney GA, Little SP, Sotiropoulou G, Becker GW, and Diamandis EP (2003). Characterization of the enzymatic activity of human kallikrein 6: Autoactivation, substrate specificity, and regulation by inhibitors. *Biochem Biophys Res Commun* **307**, 948–955.
[17] Kim JT, Song EY, Chung KS, Kang MA, Kim JW, Kim SJ, Yeom YI, Kim JH, Kim KH, and Lee HG (2011). Up-regulation and clinical significance of serine protease kallikrein 6 in colon cancer. *Cancer* **117**, 2608–2619.
[18] Ogawa K, Utsunomiya T, Mimori K, Tanaka F, Inoue H, Nagahara H, Murayama S, and Mori M (2005). Clinical significance of human kallikrein gene 6 messenger RNA expression in colorectal cancer. *Clin Cancer Res* **11**, 2889–2893.
[19] Ohlsson L, Lindmark G, Israelsson A, Palmqvist R, Oberg A, Hammarstrom ML, and Hammarstrom S (2012). Lymph node tissue kallikrein-related peptidase 6 mRNA: a progression marker for colorectal cancer. *Br J Cancer* **107**, 150–157.
[20] Qi L and Ding Y (2014). Screening and regulatory network analysis of survival-related genes of patients with colorectal cancer. *Sci China Life Sci* **57**, 526–531.
[21] Henkhaus RS, Gerner EW, and Ignatenko NA (2008). Kallikrein 6 is a mediator of K-RAS-dependent migration of colon carcinoma cells. *Biol Chem* **389**, 757–764.
[22] Ignatenko NA, Zhang H, Watts GS, Skovan BA, Stringer DE, and Gerner EW (2004). The chemopreventive agent alpha-difluoromethylornithine blocks Ki-ras-dependent tumor formation and specific gene expression in Caco-2 cells. *Mol Carcinog* **39**, 221–233.
[23] Chow TF, Crow M, Earle T, El-Said H, Diamandis EP, and Yousef GM (2008). Kallikreins as microRNA targets: an in silico and experimental-based analysis. *Biol Chem* **389**, 731–738.
[24] Gentleman RC, Carey VJ, Bates DM, Bolstad B, Dettling M, Dudoit S, Ellis B, Gautier L, Ge Y, and Gentry J, et al (2004). Bioconductor: open software development for computational biology and bioinformatics. *Genome Biol* **5**, R80.
[25] Ritchie ME, Phipson B, Wu D, Hu Y, Law CW, Shi W, and Smyth GK (2015). limma powers differential expression analyses for RNA-sequencing and microarray studies. *Nucleic Acids Res* **43**, e47.
[26] Pampalakis G, Prosnikli E, Agalioti T, Vlahou A, Zoumpourlis V, and Sotiropoulou G (2009). A tumor-protective role for human kallikrein-related peptidase 6 in breast cancer mediated by inhibition of epithelial-to-mesenchymal transition. *Cancer Res* **69**, 3779–3787.
[27] Betel D, Wilson M, Gabow A, Marks DS, and Sander C (2008). The microRNA.org resource: targets and expression. *Nucleic Acids Res* **36**, D149–D153.
[28] Betel D, Koppal A, Agius P, Sander C, and Leslie C (2010). Comprehensive modeling of microRNA targets predicts functional non-conserved and non-canonical sites. *Genome Biol* **11**, R90.
[29] Attisano L and Wrana JL (2002). Signal transduction by the TGF-beta superfamily. *Science* **296**, 1646–1647.
[30] Nieto MA (2002). The snail superfamily of zinc-finger transcription factors. *Nat Rev Mol Cell Biol* **3**, 155–166.
[31] Moes M, Le Bechec A, Crespo I, Laurini C, Halavatyi A, Vetter G, Del Sol A, and Friederich E (2012). A novel network integrating a miRNA-203/SNAI1 feedback loop which regulates epithelial to mesenchymal transition. *PLoS One* **7**, e35440.
[32] Li Y, Zhao Z, Xu C, Zhou Z, Zhu Z, and You T (2014). HMGA2 induces transcription factor Slug expression to promote epithelial-to-mesenchymal transition and contributes to colon cancer progression. *Cancer Lett* **355**, 130–140.
[33] Thuault S, Valcourt U, Petersen M, Manfioletti G, Heldin CH, and Moustakas A (2006). Transforming growth factor-beta employs HMGA2 to elicit epithelial-mesenchymal transition. *J Cell Biol* **174**, 175–183.
[34] Henkhaus RS, Roy UK, Cavallo-Medved D, Sloane BF, Gerner EW, and Ignatenko NA (2008). Caveolin-1-mediated expression and secretion of kallikrein 6 in colon cancer cells. *Neoplasia* **10**, 140–148.
[35] Valastyan S and Weinberg RA (2009). MicroRNAs: Crucial multi-tasking components in the complex circuitry of tumor metastasis. *Cell Cycle* **8**, 3506–3512.
[36] Bouyssou JM, Manier S, Huynh D, Issa S, Roccaro AM, and Ghobrial IM (2014). Regulation of microRNAs in cancer metastasis. *Biochim Biophys Acta* **1845**, 255–265.
[37] Weng M, Wu D, Yang C, Peng H, Wang G, Wang T, and Li X (2016). Noncoding RNAs in the development, diagnosis, and prognosis of colorectal cancer. *Transl Res* .
[38] Wang XF, Shi ZM, Wang XR, Cao L, Wang YY, Zhang JX, Yin Y, Luo H, Kang CS, and Liu N, et al (2012). MiR-181d acts as a tumor suppressor in glioma by targeting K-ras and Bcl-2. *J Cancer Res Clin Oncol* **138**, 573–584.
[39] Drucker KL, Paulsen AR, Giannini C, Decker PA, Blaber SI, Blaber M, Uhm JH, O'Neill BP, Jenkins RB, and Scarisbrick IA (2013). Clinical significance and novel mechanism of action of kallikrein 6 in glioblastoma. *Neuro Oncol* **15**, 305–318.
[40] Sidiropoulos KG, White NM, Bui A, Ding Q, Boulos P, Pampalakis G, Khella H, Samuel JN, Sotiropoulou G, and Yousef GM (2014). Kallikrein-related peptidase 5 induces miRNA-mediated anti-oncogenic pathways in breast cancer. *Oncoscience* **1**, 709–724.
[41] Thuault S, Tan EJ, Peinado H, Cano A, Heldin CH, and Moustakas A (2008). HMGA2 and Smads co-regulate SNAIL1 expression during induction of epithelial-to-mesenchymal transition. *J Biol Chem* **283**, 33437–33446.
[42] Tran DD, Corsa CA, Biswas H, Aft RL, and Longmore GD (2011). Temporal and spatial cooperation of Snail1 and Twist1 during epithelial-mesenchymal transition predicts for human breast cancer recurrence. *Mol Cancer Res* **9**, 1644–1657.
[43] Gregory PA, Bert AG, Paterson EL, Barry SC, Tsykin A, Farshid G, Vadas MA, Khew-Goodall Y, and Goodall GJ (2008). The miR-200 family and miR-205 regulate epithelial to mesenchymal transition by targeting ZEB1 and SIP1. *Nat Cell Biol* **10**, 593–601.
[44] Gregory PA, Bracken CP, Smith E, Bert AG, Wright JA, Roslan S, Morris M, Wyatt L, Farshid G, and Lim YY, et al (2011). An autocrine

TGF-beta/ZEB/miR-200 signaling network regulates establishment and maintenance of epithelial-mesenchymal transition. *Mol Biol Cell* **22**, 1686–1698.

[45] Benaich N, Woodhouse S, Goldie SJ, Mishra A, Quist SR, and Watt FM (2014). Rewiring of an epithelial differentiation factor, miR-203, to inhibit human squamous cell carcinoma metastasis. *Cell Rep* **9**, 104–117.

[46] Baker K, Raut P, and Jass JR (2007). Microsatellite unstable colorectal cancer cell lines with truncating TGFbetaRII mutations remain sensitive to endogenous TGFbeta. *J Pathol* **213**, 257–265.

[47] Wang X, Liu X, Li AY, Chen L, Lai L, Lin HH, Hu S, Yao L, Peng J, and Loera S, et al (2011). Overexpression of HMGA2 promotes metastasis and impacts survival of colorectal cancers. *Clin Cancer Res* **17**, 2570–2580.

[48] White NM, Youssef YM, Fendler A, Stephan C, Jung K, and Yousef GM (2012). The miRNA-kallikrein axis of interaction: a new dimension in the pathogenesis of prostate cancer. *Biol Chem* **393**, 379–389.

[49] Sidiropoulos KG, Ding Q, Pampalakis G, White NM, Boulos P, Sotiropoulou G, and Yousef GM (2016). KLK6-regulated miRNA networks activate oncogenic pathways in breast cancer subtypes. *Mol Oncol* **10**, 993–1007.

[50] Gurtan AM and Sharp PA (2013). The role of miRNAs in regulating gene expression networks. *J Mol Biol* **425**, 3582–3600.

[51] Locker GY, Hamilton S, Harris J, Jessup JM, Kemeny N, Macdonald JS, Somerfield MR, Hayes DF, and Bast Jr RC (2006). ASCO 2006 update of recommendations for the use of tumor markers in gastrointestinal cancer. *J Clin Oncol* **24**, 5313–5327.

[52] Shannon P, Markiel A, Ozier O, Baliga NS, Wang JT, Ramage D, Amin N, Schwikowski B, and Ideker T (2003). Cytoscape: a software environment for integrated models of biomolecular interaction networks. *Genome Res* **13**, 2498–2504.